Modeling Electrostatically Induced Collapse Transitions in Carbon Nanotubes

Oleg E. Shklyaev, Eric Mockensturm, and Vincent H. Crespi

Modeling electrostatically induced collapse transitions in carbon nanotubes

Oleg E. Shklyaev, Eric Mockensturm

Department of Mechanical and Nuclear Engineering,
The Pennsylvania State University, University Park, PA, 16802-6300, USA

Vincent H. Crespi

Department of Physics and Materials Research Institute,
The Pennsylvania State University, University Park, PA, 16802-6300, USA

Molecular dynamics simulations demonstrate how a mechanically bistable single-walled carbon nanotube can act as a variable-shaped capacitor with a voltage-controlled transition between collapsed and inflated states. This external control parameter provides a means to tune the system so that collapsed and inflated states are degenerate, at which point the tube's susceptibility to diverse external stimuli– temperature, voltage, trapped atoms – diverges following a universal curve, yielding an exceptionally sensitive sensor or actuator that is characterized by a vanishing energy scale. For example, the boundary between collapsed and inflated states can shift hundreds of Angstroms in response to the presence or absence of a single gas atom in the core of the tube. Several potential nano-electromechanical devices could be based on this electrically tuned crossover between near-degenerate collapsed and inflated configurations.

PACS numbers: 61.48.De, 85.85+j, 85.35.Kt, 64.70.Nd

The equilibrium cross-sectional shape of a nanotube is controlled by a competition between elastic and surface energies. Sufficiently large-diameter tubes prefer the collapsed state, which captures the surface energy of the now-touching interior surfaces. Three distinct stability regimes can be defined in terms of the radius of the inflated, cylindrical state: below R_1 only the inflated state is stable; between R_1 and R_2 the inflated state remains stable, but the collapsed state is metastable; above R_2 collapse is stable and inflation is only metastable[1–6]. In the region of bistability above R_1, transitions between these two configurations can propagate down the axis of the tube[8,9]. Here we show how the highly deformable conductive sp^2 sheet can act as a *non-linear, variable-shape capacitor* wherein electrostatic interactions within a charged tube shift R_1 and R_2 to favor the inflated state. A tube can be tuned by external voltage to a critical point at which the inflated and collapsed states are degenerate, producing a divergent susceptibility to diverse external stimuli and creating a regime of exceptionally sensitive nonlinear nano-electromechanical response.

Consider an infinitely long single-walled tube of radius R wherein an external voltage U (relative to infinity) imparts additional charge q onto the tube wall. We model the covalent interatomic interactions of this system with a Tersoff-Brenner potential[10,11], the non-bonded interactions with a Lennard-Jones term, and the electrostatic contribution via a screened Coulomb interaction and charging energy. The parameters ϵ and σ of the Lennard-Jones interaction $\phi_{LJ}(r) = \epsilon \left(\frac{\sigma}{r}\right)^{12} - 2\epsilon \left(\frac{\sigma}{r}\right)^6$ are $\sigma = 0.383$ nm and $\epsilon = 2.39$ meV[12]. Since the Lennard-Jones term describes only long-distance non-bonded interactions, we exclude sufficiently short interatomic distances ($r < 0.3$ nm) from the Lennard-Jones term, as is standard practice. For computational efficiency, we neglect non-bonded interactions for $r > r_0$ nm and shift the Lennard-Jones potential upward by a small term linear
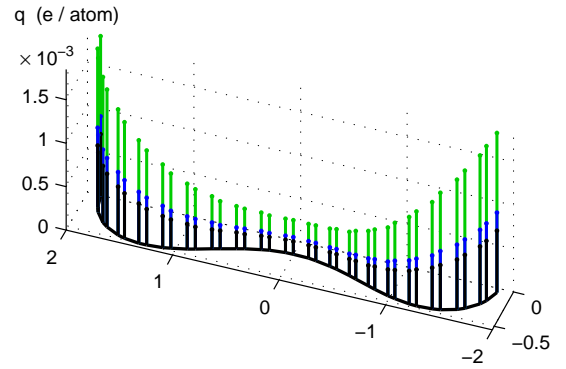

FIG. 1: Charge distribution over the collapsed configuration of (20,20) tube, showing the accumulation of charge in the bulbs. Dark blue and light green lines correspond to $U = 1$ and $U = 2$ V at $k_s = 0.1$ nm^{-1}, while black lines correspond to $k_s = 0.05$ nm^{-1} at $U = 1$ V.

in r so that the energy and force vanish at the cutoff distance[5,7]. In any real system, the induced charge on the tube wall is screened by countercharges in the environment. In addition, coarse graining of the induced charge onto atoms requires an empirical on-site Coulomb self-interaction. Hence we introduce an on-atom self-energy that is linear in the induced charge and use a Thomas-Fermi screening at long distances:

$$4\pi\epsilon_0 \phi_\Sigma(\mathbf{r}_i) = Aq_i + \sum_{j \neq i} q_j \frac{e^{-k_s \mathbf{r}_{ij}}}{\mathbf{r}_{ij}}. \qquad (1)$$

The empirical parameter $A = 7.8$ nm^{-1} is fitted to results when $k_s = 0$[13], but the precise value of A has only minor effects on our main results. Thomas-Fermi screening provides a reasonably accurate model of screening due to e.g. an electrolyte. In 10^{-1} to 10^{-4} M NaCl solutions

the Debye screening length varies from 30 to 1 nm[14]; we use $k_s = 0.2, 0.1, 0.05$ nm^{-1}. The net electrostatic self-interaction is $E_\Sigma = \frac{1}{2} \sum_{i=1}^{N} q_i \phi_\Sigma(r_i)$. At fixed applied voltage U, the tube when collapsed holds less charge than when inflated, yielding a contribution $E_Q = -qU$ due to work against this external voltage. The total energy is then a sum of covalent (E_{TB}), non-bonded (E_{LJ}), and electrostatic ($E_\Sigma + E_Q$) contributions. The energy differences ΔE quoted below are always relative to the energy of the corresponding inflated state at the same voltage, so that $\Delta E = 0$ corresponds to degeneracy. Equations of motion (under periodic boundary conditions) are integrated with a Verlet algorithm, incorporating viscous damping to relax to static equilibria.

A constant-voltage condition models a tube strongly coupled to an electrode by e.g. a highly conductive or ohmic contact; (a constant-charge condition could model a tunneling contact, with a distinct type of collapse/inflation transition dynamics described later). When the tube is collapsed, the charge accumulates in the bulbs, as shown in Fig. 1. To find the charge distribution, we write the potential $\phi_\Sigma(\mathbf{r}_i)$ given by (1) for each atom $1 \leq i \leq N$ in the unit cell and solve the system of self-consistent linear equations:

$$\sum_{j \neq i}^{j=N} q_j \sum_{n=-\infty}^{n=\infty} \frac{e^{-k_s \rho_{ijn}}}{\rho_{ijn}} + q_i \left(A + \sum_{n=-\infty}^{n=\infty}{}' \frac{e^{-k_s |nL|}}{|nL|} \right) = 4\pi \epsilon_0 \phi_\Sigma(\mathbf{r}_i),$$

with respect to unknown charges q_i at a fixed electrostatic potential $\phi_\Sigma(\mathbf{r}_i) = U$, where ρ_{ijn} is the distance between atoms i and j separated by n unit cells. The primed sum omits $n = 0$.

Fig. 1 shows the excess charge per atom. As regions of high curvature, the bulbs accumulate charge, more so at higher voltages. More weakly screened charge distributions require less total charge to sustain a given voltage. For strong screening, the on-site self-energy in Eqn. (2) is more important compared to the inter-atomic interaction, so the system becomes slightly more sensitive to the empirical parameter A[15].

The inflated state holds more charge than the collapsed state at fixed voltage, therefore it has a higher capacitance and is favored under increasing charge. The upper panel of Fig. 2 depicts voltage-controlled shape transitions for (20,20), (30,30) and (40,40) tubes. All three systems are initialized to a collapsed state at $U = 0$; (collapse is metastable for (20,20) or (30,30) and stable for (40,40)). Charging not only favors the higher-capacitance inflated state, but also decreases the barrier against inflation. At $U_{\text{crit}}(R)$ the kinetic barrier against inflation disappears and the tube inflates. The inset in the figure depicts this transition for the (40,40) tube. As the voltage increases, the bulbs expand and the flattened interior shrinks. At $U_{\text{crit}} \approx 39$ V the tube snaps open. The middle and lower panels of Fig. 2 demonstrate influence of the screening parameter k_s on the energy ΔE
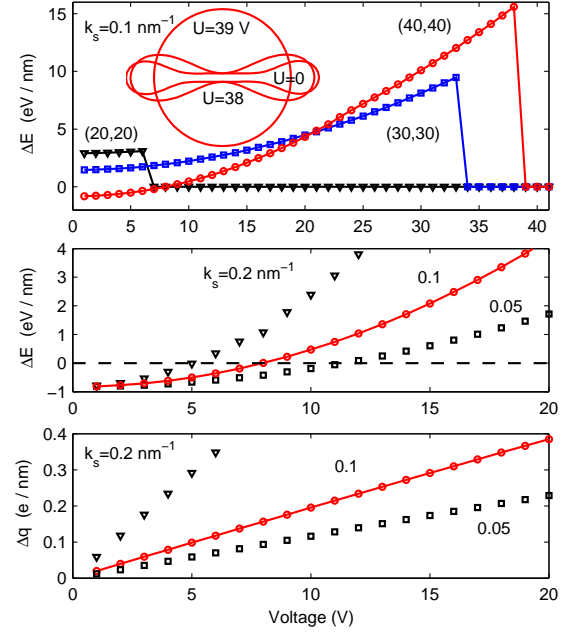

FIG. 2: Upper panel: Net energy $\Delta E = \Delta E_{TB} + \Delta E_{LJ} + \Delta E_\Sigma + \Delta E_Q$ per unit length of (20,20), (30,30) and (40,40) tubes as a function of the applied voltage U, where $\Delta E = 0$ corresponds to the inflated state at the same voltage. Discontinuities correspond to abrupt transitions into the inflated state. The inset shows changes of the shape of a (40,40) tube under external voltage. Middle panel: ΔE for a (40,40) tube when $k_s = 0.2, 0.1, 0.05$nm^{-1}. Lower panel: charge difference between the inflated and collapsed configurations for a (40,40) tube; the near-linearity indicates that the end-state tube shapes are relatively insensitive to charge (i.e. the capacitances of inflated and collapsed states are each roughly constant across this range of voltage).

and charge difference Δq correspondingly. The effect is robust across a wide range of screening lengths. Of particular interest are the more modest voltages needed to tune the system to the degeneracy point $\Delta E = 0$, a condition in which the system becomes exceptionally sensitive to external perturbations, as described below. This degeneracy and the resulting diverging response functions are robust to variations in the empirical potential or finite-temperature entropic contributions, since they arise from fundamental geometrical characteristics: the competition between elastic and electrostatic terms – which favor high-symmetry structures with uniform curvature – and surface energies – which favor low-symmetry structures with opposing surfaces in contact. Since a barrier exists between the inflated and collapsed states of the homogeneous system, inflation is not reversible unless appropriate boundary conditions are imposed, such as in the "double pinned" tube discussed below. In addition, we note that a real experimental system may show hysteresis due to charge (or dipole) trapping on the substrate underlying the tube[16,17].
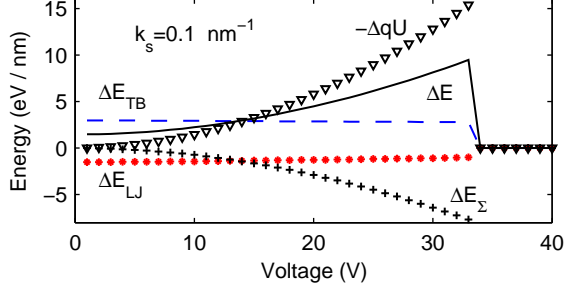
FIG. 3: Decomposition of the energy difference ΔE between collapsed and inflated states for a charged (30,30) tube into covalent/elastic (E_{TB}), Lennard-Jones (E_{LJ}), Coulomb (E_Σ), and charging (ΔqU) contributions, all measured per unit length for $k_s = 0.1\text{nm}^{-1}$.

Fig. 3 depicts the various contributions to ΔE (solid line), the energy difference between collapsed and inflated states, as functions of U for the (30,30) tube. The elastic contribution (blue dashed line) is always positive, since a uniform circular cross-section minimizes the total curvature energy. Conversely, the Lennard-Jones contribution (red dots) is always negative, since the collapsed state allows closer approach of opposing surfaces. Since the collapsed state has a lower capacitance, the Coulomb self-energy ΔE_Σ (pluses) is negative (at fixed voltage). The charging contribution ΔE_Q (triangles) associated with motion of excess charge on or off the tube is positive, due to the same difference in capacitance.

For tubes with $R > R_2$, like (40,40), the external voltage can be tuned so that collapsed and inflated states are degenerate, i.e. $\Delta E = 0$. Since this $U_{\text{degen}} < U_{\text{crit}}$, the two states are separated by a barrier. If boundary conditions that eliminate this barrier are imposed, then the susceptibility against perturbations that favor collapse or inflation will *diverge* at this critical voltage. For example, a tube with $R > R_2$ held inflated at one end and collapsed at the other (as shown in Fig. 4) must contain a transition region. The kinetic barrier between degenerate configurations is thereby eliminated. Such pinning has already been produced experimentally, even in the first paper on nanotube collapse[1], since the rigid end-cap of a tube holds the end of the tube open even after the interior collapses. This pinned-open/pinned-closed configuration provides many possible modes of device operation, which either operate *around* the degeneracy point and *at* it.

Devices that operate *around* the degeneracy point: By sweeping the applied voltage across U_{degen}, a doubly pinned nanotube can act as a electrical-mechanical transducer, transitioning between the two states shown in Fig. 4. In actuator mode, the inflating tube could perform work over long axial distances (by pushing a load along the axis) or short transverse distances (limited by the tube diameter). Axial motions could couple to either liquids inside the tube or solids attached to the tube exterior. Reversing the transduction, the system could

FIG. 4: Schematic depicting the evolution of a double-pinned tube from a mostly collapsed state at $U < U_{\text{degen}}$ to a mostly inflated state at $U > U_{\text{degen}}$.

also convert mechanical motion into charge, similar to a piezoelectric sensor. Since the collapsed state has the smaller capacitance, a charge Δq will leave the tube when a compressive load collapses the tube. For example, approximately 200 eV of work will collapse a 100 nm length of a (40,40) tube held at $U = 15$ V (for $k_s = 0.1$), producing a charge signal of $\Delta q \sim 30e$, (Fig. 2) which is easily measurable[22-24]. Unlike piezoelectric crystals whose fractional capacity to elongate $\Delta l/l$ is at most $\sim 10^{-3}$, bistable nanotube devices – for axial transport – can have a range of motion comparable to the length of the device. The efficiency of this transducer varies considerably depending on the operating voltage, but is comparable to that of established piezoelectric actuators[25].

The time response of these nonlinear nano-mechanical systems is governed by the axial speed of the transition front between collapsed and inflated states. This front moves at $v \propto \sqrt{\Delta E}$[8,9]; in our system ΔE is proportional to the voltage deviation from U_{degen}. For example, a ten-volt swing away from U_{degen} for a (40,40) tube yields $\Delta E_a \sim 2$ meV per carbon atom; taking m_C as a characteristic mass, one obtains $v \sim \sqrt{\Delta E_a/m_C} \sim 200$ m/s. A typical device dimension of 0.1 micron then implies roughly GHz operating frequencies.

Devices that operate *at* the degeneracy point: Of particular interest are devices designed to operate as close to degeneracy as possible. Such a system is very sensitive to external perturbations that upset the balance between inflated and collapsed states. For example, a gas trapped in the interior adds a PV term to the free energy (tube buckling under hydrostatic pressure is discussed in[8]), so that equilibrium is obtained when the gas pressure balances the energy density associated with the volume change between collapsed and inflated states: $P = \Delta E/\Delta A$ where ΔA is a change in the cross section area and ΔE is measured per unit axial length; (this simple analysis neglects fluctuations, which are discussed later). For an ideal gas, one obtains the differential sensitivity of the length x of the inflated portion to changes in either atom number n or temperature T:

$$\Delta x = -\frac{nk_B\Delta T}{\Delta E} = -\frac{k_BT\Delta n}{\Delta E}. \qquad (3)$$

Tuning the voltage to U_{degen}, we obtain $\Delta x \to \infty$. A single interior gas atom could shift the transition zone by a substantial amount, limited by the precision with which the energetics can be tuned. Expanding $\Delta E(U)$ around $U = U_{\text{degen}}$ for a (40,40) tube with $k_s = 0.1$, we can obtain the response functions to temperature ($\Delta x/\Delta T$) or atom number ($\Delta x/\Delta n$) as a universal family of curves plotted in Fig. 5. These curves are interpretable as either the sensitivity to temperature at fixed number of inte-
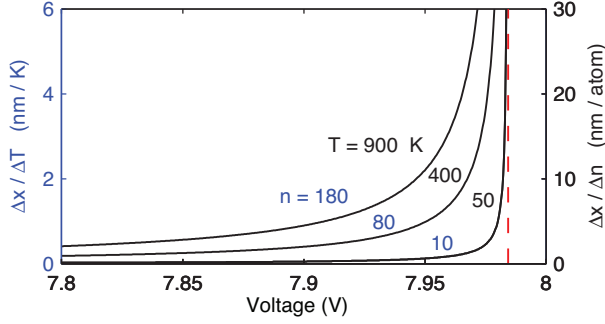
FIG. 5: Universal response function to temperature $\Delta x/\Delta T$ (or atom number $\Delta x/\Delta n$) for different number of encapsulated atoms n (or temperature T). The red dashed line marks U_{degen}.

rior gas atoms or the sensitivity to atom number at fixed temperature. Other external perturbations can also elicit strong responses: for example, dramatic responses can be anticipated to surface acoustic wave excitation, a nonlinear version of the nanotube charge pumping that was previously examined[26] for regular inflated tubes. Adsorbates and variations in temperature[27] or mechanical boundary conditions provide additional experimental handles to tilt the delicate balance between configurational states.

Collapsed-based nano-electromechanical devices could also be operated in constant-charge mode rather than constant-voltage mode, a distinction similar to that between constant-pressure and constant-volume. At constant charge the qU term is absent but the inflated state continues to be favored at higher charge per unit length.

Around the degeneracy point the system self-organizes into a mixed collapsed/inflated state, with higher charge density in the inflated section than in the collapsed one. This charge bubble – a giant polaron of sorts – could be subject to further experimental manipulation through scanned probes or split gates.

Although huge, tunable responses to perturbations are possible in this system, non-uniformities along the tube will prevent perfect tuning and hence cut off the divergent susceptibility. For example, voltage fluctuations of $\delta U = 10$ mV are characteristic of nanotubes or graphene on silica substrates[28] (with more uniform environments on alternative substrates[29]). An inhomogeneity of $\delta U = 10$ mV cuts off dX/dn at ~ 18 nm/atom at $T = 400$ K. Thermal fluctuations should be particularly important in this nanoscale, one-dimensional system. A simple one-degree-of-freedom model (which assumes a constant shape to the transition region) writes the energy of the system as ΔEx where x is the location of the collapse-inflation transition, yielding $\sqrt{\langle x^2\rangle - \langle x\rangle^2} = \frac{kT}{\Delta E}$. Since the system has only one characteristic length scale, the same universal divergence results, with fluctuations in the location of the collapse/inflation transition of the same size as the increment in location induced by a single additional interior gas atom (Eqn. 3b). This distance can be many nanometers and could be exploited in fluctuation-based device modalities similar to those of biological molecular motors.

[1] N. G. Chopra, L. X. Benedict, V. H. Crespi, M. L. Cohen, S. G. Louie, A. Zettl, Nature **377**, 135 (1995).

[2] L. X. Benedict, V. H. Crespi, N. G. Chopra, A. Zettl, M. L. Cohen, S. G. Louie, Chem. Phys. Lett. **286**, 490 (1998).

[3] G. Gao, T. Cagin, W. A. Goddard, Nanotechnology **9**, 184 (1998).

[4] T. Tang, A. Jagota, C.-Y. Hui, N. J. Glassmaker, J. Appl. Phys. **97**, 074310 (2005).

[5] S. Zhang, R. Khare, T. Belytschko, K. J. Hsia, S. L. Mielke, G. C. Schatz, Phys. Rev. B **73**, 075423 (2006).

[6] E. Mockensturm, A. Mahdavi, V. Crespi, Proc. of IMECE 2005, 82991 (2005).

[7] Following[5], the cutoff distance r_0 was chosen close to 1 nm.

[8] B. I. Yakobson, C. J. Brabec, J. Bernholc, J. Comput.-Aided Mater. Des. **3**, 173 (1996)

[9] T. Chang, Phys. Rev. Lett. **101**, 175501 (2008).

[10] D. W. Brenner, Phys. Rev. B **42**, 9458 (1990).

[11] The Tersoff-Brenner potential underestimates the bending stiffness of an sp^2 sheet: writing the strain energy of a nanotube as $D'/(2R)^2$,[18] one obtains $D' = 0.08, 0.046$ eV nm^2/atom for first-principles density functional theory[19,20], and the first generation[20,21] Tersoff-Brenner potentials, respectively. To simplify numerical simulations, we adopt the first-generation potential (the capabilities of the second-generation potential regarding close atomic ap-proaches are not needed here). This underestimation of the bending stiffness does not change any of our main conclusions, but it does shift all of the stability regimes towards smaller radii.

[12] L. A. Girifalco, M. Hodak, R. S. Lee, Phys. Rev. B **62**, 13104 (2000).

[13] P. Keblinski, S. K. Nayak, P. Zapol, P. M. Ajayan, Phys. Rev. Lett. **89**, 255503 (2002).

[14] J. Lyklema (1993). Fundamentals of interface and colloid science. Academic press, NY.

[15] In computations performed for (20,20) tube at $U = 5$ V, a ten percent variance in $A = 7.8$nm^{-1} produced less than 1% errors in relative tube energy, ΔE, for $k_s = 0.1, 0.05, 0.025$ nm^{-1}.

[16] W. Kim, A. Javey, O. Vermesh, Q. Wang, Y. Li, H. Dai, Nano Lett. **3**, 193 (2003).

[17] M. Lafkioti, B. Krauss, T. Lohmann, U. Zschieschang, H. Klauk, K. v. Klitzing, J. H. Smet, Nano Lett. **10**, 1149 (2010).

[18] G. G. Tibbetts, J. Crys. Growth **66**, 632 (1983).

[19] D. Sanchez-Portal, E. Artacho, J. M. Soler, A. Rubio, P. Ordejon, Phys. Rev. B 59, 12678 (1999)

[20] B. I. Yakobson, P. Avouris, Top. Appl. Phys. **80**, 287 (2001).

[21] D. H. Robertson, D. W. Brenner, J. W. Mintmire, Phys.

Rev. B **45**, 12592 (1992)

[22] J. Bylander, T. Duty, P. Delsing, Nature, **434**, 361, (2005).

[23] M. W. Keller, J. M. Martins, N. M. Zimmerman, A. H. Steinbach, Appl. Phys. Lett. **69** (12), 1804, (1996).

[24] H. Grabert, M. H. Devoret, Single Charge Tunneling: Coulomb Blockade Phenomena in Nanostructures (Plenum, New York, 1992)

[25] S. O. Moheimani, A. J. Fleming, (2006) Piezoelectric transducers for vibration control and damping. Springer.

[26] V. I. Talyanskii, D. S. Novikov, B. D. Simons, L. S. Levitov, Phys. Rev. Lett. **87** (27), 276802, (2001); V. I. Talyanskii, P. Leek, M. Buitelaar, C. G. Smith, D. Anderson, J. Jones, J. Wei, D. Cobden, Physica E **34**, 662, (2006).

[27] T. Chang, Z. Guo, Nano Lett. **10**, 3490 (2010).

[28] J. Martin, N. Akerman, G. Ulbright, T. Lohmann, J. H. Smet, K. von Klitzing, A. Yacoby, Nature, Physics, **4**, 144 (2008).

[29] X. Hong, A. Posadas, K. Zou, C. H. Ahn, J. Zhu, Phys. Rev. Lett. **102**, 136308 (2009).